Noseleaf Furrows in a Horseshoe Bat Act as Resonance Cavities Shaping the Biosonar Beam

Qiao Zhuang

School of Information Science and Engineering, Shandong University, Shanda Nanlu 27, 250100 Jinan, China

Rolf Müller[*]

School of Physics and Microelectronics, Shandong University, Hongjia Lou 5, 250100 Jinan, China
(Received 22 July 2006; published 22 November 2006)

Horseshoe bats emit their ultrasonic biosonar pulses through nostrils surrounded by intricately shaped protuberances (noseleaves). While these noseleaves have been hypothesized to affect the sonar beam, their physical function has never been analyzed. Using numerical methods, we show that conspicuous furrows in the noseleaf act as resonance cavities shaping the sonar beam. This demonstrates that (a) animals can use resonances in external, half-open cavities to direct sound emissions, (b) structural detail in the faces of bats can have acoustic effects even if it is not adjacent to the emission sites, and (c) specializations in the biosonar system of horseshoe bats allow for differential processing of subbands of the pulse in the acoustic domain.

PACS numbers: 43.80.+p

Like all (micro)bats, horseshoe bats use a biosonar system. Specifically, they emit ultrasonic pulses through the nostrils and listen to the returning echoes. The approximately 130 different horseshoe bat species derive their common name from fleshy protrusions—so-called "noseleaves"—which surround the nostrils. Noseleaves are a common anatomical feature in bats. Besides horseshoe bats, they are also found in the second largest family of bats, the new-world leaf-nosed bats (*Phyllostomidae* [1]), as well as in several smaller groups. While noseleaves have been frequently hypothesized to affect the angular distribution of the emitted sound energy [2], the experimental pilot data collected so far have been scarce and limited to observations from coarse, poorly controlled manipulations: The impact of tilting back an entire noseleaf has been studied in a single species belonging to the new-world leaf-nosed bats, where the natural position of the noseleaf was found to narrow the vertical width of the sound beam [3]. In another study [4], a change in beam shape was observed when the entire upper portion of a horseshoe bat's noseleaf was covered with petroleum jelly. The latter results are difficult to interpret, however, because multiple shape features may have been affected. The noseleaves of horseshoe bats are elaborate structures consisting of three parts: a smooth baffle ("horseshoe") which fills approximately the bottom three-quarters of a circle around the nostrils, a forward-pointing central spike (sella) which is adjacent to the upper rim of the nostrils, and a pointed flap ("lancet") which is located above the sella. The lancet is unique because it is the only part of the noseleaf not immediately adjacent to the nostrils and its surface is grooved with a set of horizontal furrows, which have already been depicted in [5] more than 100 years ago. Together with other morphological features responsible for the complexity of these shapes, the furrows are also widely used to distinguish different horseshoe bat species [6]. But despite their long-known, striking appearance and

taxonomic use, the question whether the furrows have a physical function or are mere decorations has remained unstudied. Besides their noseleaves, horseshoe bats also feature a conspicuous biosonar pulse design (Fig. 3, inset) which combines a comparatively long narrow-band ["constant frequency" (CF)] portion with a frequency-modulated (FM) portion. So-called "CF-FM" bats with this pulse design are model organisms in physical ecology and neuroethology [7] because of the well-studied match between sensory function and ecological niche (prey detection in clutter) and the pertinent evolutionary implications [8–10]. For a more complete understanding of this model system, it is important to know if the conspicuous morphological specializations of the noseleaves serve a function in the animals' biosonar system and how such a function may fit in. In this Letter we show that the horizontal furrows in the lancet of one horseshoe bat species, the rufous horseshoe bat, act as half-open acoustic resonance cavities. Using numerical methods (finite-element analysis), we have demonstrated the spatial and spectral specificity of the increased sound field amplitudes required as experimental evidence for a cavity resonance. Furthermore, our methods allow us to quantitatively describe the impact of the furrow resonances on the directivity function, i.e., the distribution of sound energy with direction, without any confounding additional changes to the geometry. In these results, the resonance amplitude correlates with the extent to which the directivity function is changed at different frequencies, which allows us to link the physical effect (cavity resonance) to the functionally relevant system property (the directivity function). Our results are relevant to the development of a wider understanding of the physical principles employed by bats and other animals to direct the sound energy they emit: While the use of internal resonance cavities in shaping the frequency transfer function of bioacoustic systems (e.g., in speech production) is well documented, the use of external resonance furrows to

shape the spatial transfer function reveals the exploitation of a more diverse set of principles. We show that facial features in bats can shape the sonar beam, even if they are not directly adjacent to the sound emission sites. This opens the possibility that many of the intriguing facial features seen across the approximately 1000 bat species could be acoustic devices with a physical function. The resonance frequencies of the noseleaf furrows themselves are remarkable because they differ from the frequencies all previously known specializations in these animals pertain to. This suggests that the animals have specialized processing for different frequencies in their pulses implemented by means of physical effects in the acoustic domain.

We have obtained a digital three-dimensional shape representation of the noseleaf of the rufous horseshoe bat (*Rhinolophus rouxi*) by using microcomputer tomography. This representation was converted into a finite-element model with linear cubic elements [edge length: 120 μm; Fig. 1(a)]. With studied wavelengths ranging from 3.8 to 11.4 mm, this corresponds to spatial resolutions from 32 to 95 finite elements per wavelength. Using the finite-element model, we found a numerical harmonic solution to the Helmholtz differential equation

$$\boldsymbol{\nabla}^2 \Phi + k^2 \Phi = -b, \qquad (1)$$

where Φ is the sound pressure, $k = \frac{2\pi f}{c}$ the wave number, and b the force term representing sources. The entries in the resulting element stiffness matrices $K_{ij}^{(\mathrm{el})}$ were deter-
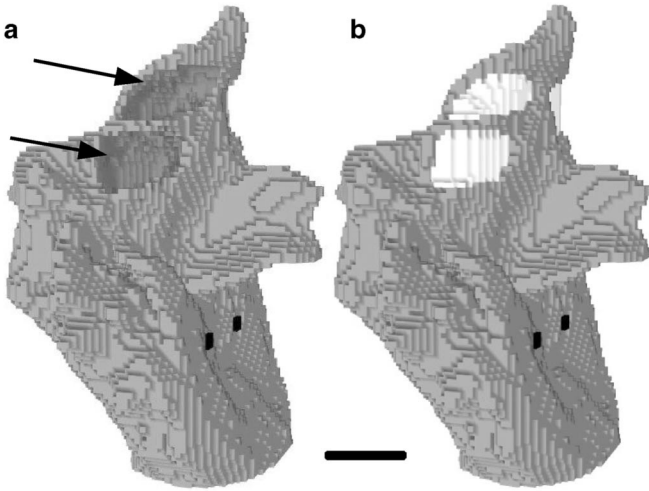
FIG. 1. Noseleaf boundary of the finite-element mesh on which the numerical calculations were carried out. (a) Mesh boundary of the representation of the natural shape of the nose-leaf: the location of the point sources is marked by black voxels; the inner surfaces of the lancet furrows (arrows) are marked by dark gray voxels. (b) Mesh boundary for the modified shape with filled-in lancet furrows: the voxels representing added material are rendered in white; the remainder of the mesh boundary and the location of the sources remained unchanged. The length of the scale bar is 2 mm.

mined analytically by evaluating the expression

$$
\begin{aligned}
K_{ij}^{(\mathrm{el})} &= \Delta K_{ij}^{(\mathrm{el})} - k^2 \Delta M_{ij}^{(\mathrm{el})} \\
&= \int_{V^{(\mathrm{el})}} \boldsymbol{\nabla} N_i^T \boldsymbol{\nabla} N_j - k^2 N_i N_j dV, \qquad (2)
\end{aligned}
$$

where $\Delta K_{ij}^{(\mathrm{el})}$ is the stiffness term, $\Delta M_{ij}^{(\mathrm{el})}$ the mass term, N_i the ith shape function, and $V^{(\mathrm{el})}$ the volume of the element. Both stiffness and mass terms are independent of frequency, and the element stiffness matrix is invariant with respect to the position of the finite element in the mesh.

The cuboidal spatial domain in which the finite-element calculations were carried out was chosen to enclose the noseleaf shape, leaving several elements representing air in each direction. On the boundary of the finite-element domain, reflection-free outward sound propagation was modeled by a layer of three-dimensional mapped wave-envelope infinite elements [11]. The entries in the element stiffness matrix of the infinite elements are given by

$$K_{ij}^{(\mathrm{el})} = \Delta K_{ij}^{(\mathrm{el})} - k^2 \Delta M_{ij}^{(\mathrm{el})} + jk\Delta C_{ij}^{(\mathrm{el})}, \qquad (3)$$

where j is the imaginary unit and $\Delta C_{ij}^{(\mathrm{el})}$ the damping term. In the radial direction, Jacobi polynomials of order three with parameters $\alpha = 2$ and $\beta = 0$ were used as basis function as suggested by [12]. The shape functions for the infinite elements were integrated numerically using Gauss-Legendre quadrature.

Two point sources were placed at single element nodes in the opening of the nostrils (Fig. 1) by assigning nonzero values to the appropriate elements in the right-hand side vector of the Helmholtz equation [Eq. (1)]. The resulting well-posed linear problem was solved iteratively for the complex wave-field amplitudes using a biconjugate gradient stabilized method [13,14] with a successive over-relaxation preconditioner implemented in the Portable, Extensible Toolkit for Scientific Computation (PETSC) software library [15].

The wave-field estimates on the outer layer of finite-element nodes were projected to a set of points on the surface of a sphere in the far field in order to obtain the normalized directivity pattern $0 \le D(\phi, \theta, f) \le 1$, i.e., the relative gain of the noseleaf as a function of azimuth ϕ, elevation θ, and frequency f which is valid for all distances in the far field [16]. The far-field projection was carried out using the Kirchhoff integral [17,18]

$$\Psi(\vec{\mathbf{x}}) = -\frac{1}{4\pi} \int_S \frac{e^{jkR}}{R} \vec{\mathbf{n}} \cdot \left[\boldsymbol{\nabla}\Psi + jk\left(1 + \frac{j}{kR}\right)\frac{\vec{\mathbf{R}}}{R}\Psi \right] ds, \qquad (4)$$

where $\vec{\mathbf{R}}$ is the vector between the surface element ds and the position $\vec{\mathbf{x}}$, $\vec{\mathbf{n}}$ is the outward-pointing surface normal, Ψ the field value on S, and k the wave number. The product $\vec{\mathbf{n}} \cdot \boldsymbol{\nabla}\Psi = \frac{\partial \Psi}{\partial \vec{\mathbf{n}}}$ is the derivative of the field Ψ with respect to the surface normal $\vec{\mathbf{n}}$.

The near-field sound pressure amplitude field showed pronounced local maxima inside the air volumes contained by the lancet furrows (Fig. 2). The amplitude values reached in these spatial maxima depended strongly on frequency (Fig. 3): a global maximum was found to exist around 60 kHz for both the lower and the upper furrow. Above and below this frequency, the amplitude showed a strong general trend to decrease with increasing distance from the maximum. The spatial and spectral dependence of this effect is a clear indication of a resonance cavity [19], for which it can be expected that the amplitude is increased only inside the cavity and that the resonance is limited to frequencies where reinforcement between the incident and reflected waves occurs. The wavelengths corresponding to the experimentally determined resonance frequencies around 60 kHz (5.7 mm) are approximately 4 times as large as the depth (and height) of the furrows (approximately 1.4 mm). This finding is in fairly good agreement with the resonance frequency of a cylindrical tube which is open on one side and closed on the other [20]. It should be pointed out, however, that the cross section of the furrows is not circular and hence modeling them as a cylindrical tube can only be regarded as a first approximation, despite the good match of the numbers in this particular case.

Since horseshoe bats use their biosonar system to detect and track insect prey as well as to avoid obstacles from a distance, the resonances inside the lancet furrows are not directly functionally relevant system features by themselves. Relevant for these biological tasks is the system behavior in the far field, which is described completely by the directivity function. The impact of the furrows on the directivity pattern was experimentally assessed by filling the furrows in the three-dimensional digital representation of the noseleaf shape by hand [Fig. 1(b)]. This experimental manipulation caused changes to the directivity patterns at all frequencies within the band used by the animal, but to an extent which depended strongly on frequency: the amount of change caused showed a maximum for the same frequency as the resonances (Fig. 3). This supports the notion that the functional properties (directivity) are linked to the structural features (furrows) by virtue of the acoustic resonances in the furrows. The maximum change to the directivity pattern was substantial and amounted to about 25% of the maximum value of the directivity function. Whereas the small changes which where observed away from the resonance frequency did not reveal a clear pattern, the large changes around the resonance frequency led to an expansion in the set of directions with maximum pulse energy along the elevation axis, in particular, upwards (Fig. 4). It is interesting to note that the resonances primarily affect the lower portion of the FM component of the biosonar pulse (from 60.4 to 81.5 kHz in the studied individual), whereas all well-known specializations in CF-FM bats—e.g., with respect to cochlear [21] and neural signal processing [7] as well as behavior [22])—are geared towards the CF portion (at 81.5 kHz in the studied individual). This supports the view that the FM portions of the pulse—rather than being appendages of

FIG. 2 (color online).　Spatial selectivity of the resonance: sound pressure amplitude (magnitude of the time-harmonic solution to the Helmholtz equation) for 60 kHz in the near field coded by gray (color) value on a linear scale. Arrows indicate the local spatial maxima inside the lancet furrows.
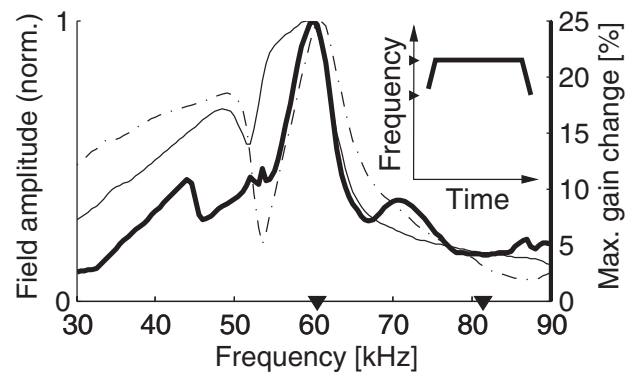
FIG. 3.　Frequency selectivity of the resonance: normalized sound pressure amplitudes in the lower (dashed line) and upper (thin solid line) right lancet furrow as a function of frequency. The frequency band displayed extends beyond the range known to be used by the bat (marked by downward triangles) in order to show the resonance behavior unequivocally. The spacing of the data points is 500 Hz, and the resonance amplitude value at each frequency was estimated based on 20 (lower furrow) or 19 (upper furrow) sample nodes located within a sphere of 0.2 mm radius; the maximum normalized standard deviation for these samples was 0.03. Superimposed on the resonance curves is the maximum change in the directivity function relative to its global maximum in percent (thick solid line). The inset shows a schematic spectrogram of a CF-FM biosonar pulse; spectrograms of pulses measured in *Rhinolophus rouxi* are given in [25].
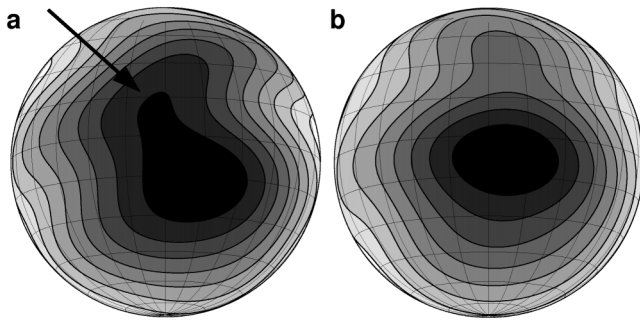
FIG. 4.   Orthographic map projections of the numerical estimates of the directivity function at 60 kHz. (a) For the unaltered noseleaf shape [Fig. 1(a)]; the arrow indicates the location of the upward extension of the beam. (b) For a modified noseleaf with all lancet furrows filled [Fig. 1(b)]. The amplitude of the directivity function is linearly encoded by the gray scale, where black represents the maximum value. Contour lines are spaced 10% of the range apart. The contour estimates are based on 65 160 function values (resolution of 1° in azimuth and elevation) each.

limited use—serve as integral, functional components of the biosonar system. Prior evidence for the functional relevance of the FM portions has come from behavioral observations of context-dependent signal variability in the animals [23]. The present results show that the use of the FM portions is also facilitated by at least one specific acoustical adaptation in the noseleaf. The frequency-selective nature of the resonance presents the bats with an opportunity for generating different beam patterns for the FM and CF portions of their pulses: At the frequency of the CF portion, the system properties are largely unaffected by the lancet furrows, and the noseleaf may act, for instance, to achieve maximum focusing of the beam, whereas in the lower subband of the FM portion, the furrow resonances shape the beam pattern and increase the extent of the beam in elevation. An asymmetric widening of the beam in a subband of the biosonar pulse is also seen in the big brown bat (*Eptesicus fuscus*), where the relative position of the tragus and pinna controls the extension of an asymmetric side lobe [24]. Both bat species may use these beam patterns in comparable strategies to direct their spatial sensitivity mainly in one direction and at the same time still allocate some sensitivity to monitoring echo returns from a different direction. Since the rufous horseshoe bat is known to fly low over ground [25], the beam widening in elevation by resonances in the lancet furrows may be interpreted as an adaptation to monitoring the ground in order to maintain a constant height and avoid ground collisions.

*Electronic address: mueller@sdu.edu.cn

[1] W. Bogdanowicz, R. Csada, and M. Fenton, J. Mammal. **78**, 942 (1997).

[2] R. M. Nowak, *Walker's Mammals of the World* (Johns Hopkins University Press, Baltimore, MD, 1991), 5th ed.

[3] D. J. Hartley and R. A. Suthers, J. Acoust. Soc. Am. **82**, 1892 (1987).

[4] H.-U. Schnitzler and A. D. Grinnell, J. Comp. Physiol. A **116**, 51 (1977).

[5] E. Haeckel, *Kunstformen der Natur* (Verlag des Bibliographischen Instituts, Leipzig, 1899).

[6] K. F. Koopman, *Chiroptera: Systematics* (de Gruyter, Berlin, 1994).

[7] C. F. Moss and S. R. Sinha, Curr. Opin. Neurobiol. **13**, 751 (2003).

[8] J. A. Simmons and R. A. Stein, J. Comp. Physiol. **135**, 61 (1980).

[9] H. Arita and M. Fenton, Trends Ecol. Evol. **12**, 53 (1997).

[10] G. Jones and E. C. Teeling, Trends Ecol. Evol. **21**, 149 (2006).

[11] R. J. Astley and G. J. Macaulay, J. Acoust. Soc. Am. **103**, 49 (1998).

[12] D. Dreyer and O. von Estorff, Int. J. Numer. Methods Eng. **58**, 933 (2003).

[13] R. Barrett, M. Berry, T. F. Chan, J. Demmel, J. Donato, J. Dongarra, V. Eijkhout, R. Pozo, C. Romine, and H. V. der Vorst, *Templates for the Solution of Linear Systems: Building Blocks for Iterative Methods* (SIAM, Philadelphia, PA, 1994), 2nd ed.

[14] H. A. van der Vorst, *Iterative Krylov Methods for Large Linear Systems*, Cambridge Monographs on Applied and Computational Mathematics Vol. 43 (Cambridge University Press, Cambridge, England, 2003).

[15] S. Balay, W. D. Gropp, L. C. McInnes, and B. F. Smith, in *Modern Software Tools in Scientific Computing*, edited by E. Arge, A. M. Bruaset, and H. P. Langtangen (Birkhäuser Press, Boston, MA, 1997), pp. 163–202.

[16] R. J. Urick, *Principles of Underwater Sound* (McGraw-Hill, New York, 1983), 3rd ed.

[17] D. E. Jackson, *Classical Electrodynamics* (John Wiley & Sons, New York, 1999), 3rd ed.

[18] O. M. Ramahi, IEEE Trans. Antennas Propag. **45**, 753 (1997).

[19] T. D. Rossing and N. H. Fletcher, *Principles of Vibration and Sound* (Springer-Verlag, New York, 2004), 2nd ed.

[20] N. H. Fletcher, *Acoustic Systems in Biology* (Oxford University Press, New York, 1992).

[21] M. Kössl, Hear. Res. **72**, 59 (1994).

[22] H.-U. Schnitzler, J. Comp. Physiol. **82**, 79 (1973).

[23] B. Tian and H.-U. Schnitzler, J. Acoust. Soc. Am. **101**, 2347 (1997).

[24] R. Müller, J. Acoust. Soc. Am. **116**, 3701 (2004).

[25] G. Neuweiler, W. Metzner, U. Heilmann, R. Rübsamen, M. Eckrich, and H. Costa, Behav. Ecol. Sociobiol. **20**, 53 (1987).